Upsilon point in a spin model

C. Micheletti
Theoretical Physics, Oxford University, 1 Keble Road, Oxford OX1 3NP, United Kingdom

F. Seno
INFM–Dipartimento di Fisica "G. Galilei," Via Marzolo 8, I-35131 Padova, Italy

J. M. Yeomans
Theoretical Physics, Oxford University, 1 Keble Road, Oxford OX1 3NP, United Kingdom
(Received 30 March 1995)

We present analytic evidence for the occurrence of an upsilon point, an infinite checkerboard structure of modulated phases, in the ground state of a spin model with uniaxial modulation. The structure of the upsilon point is studied by calculating interface-interface interactions using an expansion in inverse spin anisotropy.

I. INTRODUCTION

Simple spin models can have surprisingly complex phase structures, even at zero temperature. In particular, near multiphase lines, along which the ground state is infinitely degenerate, a perturbation such as temperature,[1] quantum fluctuations,[2] or softening of the spins[3] can result in infinite sequences of stable phases.

The existence of upsilon points (Υ points) in Frenkel-Kontorova models has been pointed out recently.[4,5] These occur when two multiphase lines meet at a first-order boundary. A small perturbation about such a point can stabilize an infinite checkerboard structure of commensurate phases as shown in Fig. 1. In many ways the Υ point can be thought of as a two-dimensional generalization of the behavior customary near a multiphase point.

The occurrence of an Υ point in a spin model was recently suggested by the numeric work of Sasaki.[6] Here we present analytic evidence for the existence of an Υ point in a spin model. The system we consider is the chiral XY model with sixfold spin anisotropy in a magnetic field.[7] We identify a candidate for an Υ point at infinite spin anisotropy D and show that, as D is reduced from infinity, the softening of the potential wells allows formation of a Υ-point structure.

We follow the method introduced by Fisher and Szpilka[8] and extended by Bassler, Sasaki, and Griffiths[9] and identify the multiphase structures as comprising interfaces separating domains of the different phases. The behavior near a single multiphase point can be analyzed in terms of a unique type of interface. However, there are two (or more) different phases stable near an Υ point and hence different types of interface must be identified in the analysis. It is the interactions between the interfaces which are responsible for breaking the multiphase degeneracy and a knowledge of their sign and dependence on separation allows determination of the phase diagram. Here the interface-interface interactions are calculated using an expansion in D^{-1}.[3]

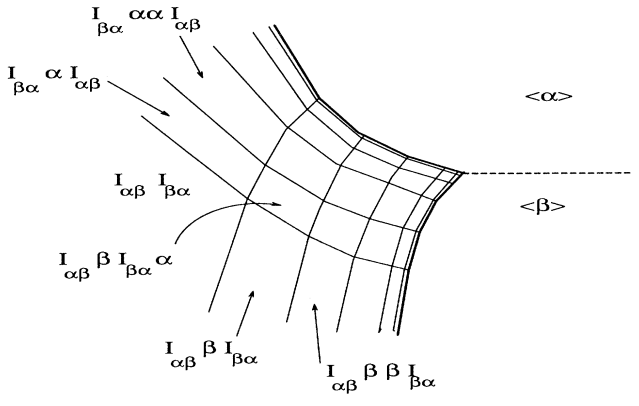

FIG. 1. Schematic representation of an Υ point. Finer details are not shown.

II. MODEL

We consider the classical chiral XY model with sixfold spin anisotropy, D, in the presence of an external magnetic field h. The Hamiltonian of the system is

$$\mathcal{H} = \sum_i \Big\{ -\cos(\theta_{i-1} - \theta_i + \pi\Delta/3) + h[1 - \cos(\theta_i)] + D[1 - \cos(6\theta_i)]/36 \Big\}, \tag{2.1}$$

where θ_i is the angle between the ith spin and the magnetic-field orientation. We shall concentrate on the behavior of the model near the limit $D = \infty$, where n_i, defined as $3\theta_i/\pi$, can take only the integer values

$\{0,1,...,5\}$. Although we restrict ourselves to one dimension the results apply equally to models with ferromagnetically coupled layers and an uniaxial modulation driven by the interactions (2.1) perpendicular to the layers.

The ground-state configurations of the Hamiltonian (2.1) satisfy

$$\frac{\partial \mathcal{H}}{\partial \theta_i} = 0 \quad \forall i. \tag{2.2}$$

For a given i, Eq. (2.2) enables us to express θ_{i+1} as a function of θ_i and θ_{i-1}. This fact, together with the observation that $n_i \in \{0, 1, ..., 5\}$, is sufficient to conclude that, for $D = \infty$, there will always exist periodic minimal energy configurations. It will be convenient to label a periodic configuration $\{..., \theta_N, \theta_1, \theta_2, ..., \theta_N, \theta_1, ...\}$ as $\langle n_1\, n_2 \ldots n_N \rangle$.

We can now discuss the phase diagram for $D = \infty$, obtained using the Floria-Griffiths algorithm,[10] and presented in Fig. 2. We have restricted the labeling of the phases to the first quadrant ($0 \leq \Delta \leq 3; h \geq 0$); the remaining phases can be constructed through appropriate symmetry operations on the n_i sequences. The transition lines between regions A and J and regions J and F are first order. The remaining boundaries are multiphase lines, that is loci where all phases (including nonperiodic ones) built from arbitrary combinations of the two neighboring phases are degenerate.[1]

If the spin anisotropy is reduced from ∞ it seems natural to expect the degeneracy along the multiphase lines to be lifted as the spins soften from the clock positions. Although n_i is no longer constrained to assume integer values, nevertheless, for high values of D, the angles θ_i will be close enough to the clock positions to allow us to continue to use the same labeling scheme.

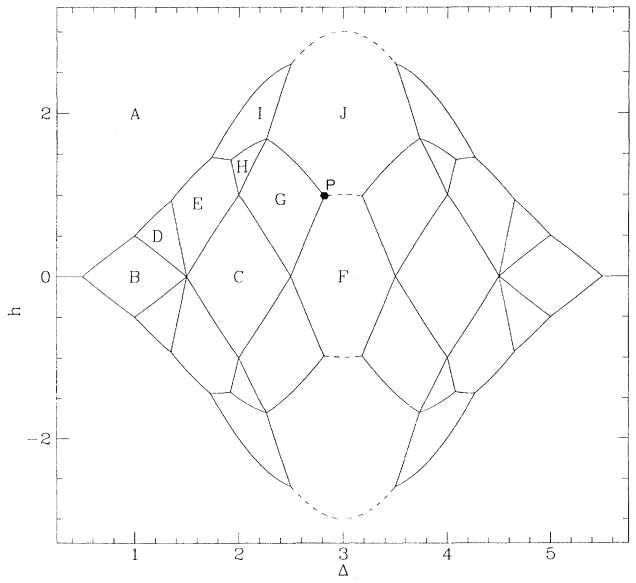

FIG. 2. Ground state of the Hamiltonian (2.1) for $D = \infty$. $A = \langle 0 \rangle$; $B = \langle 012345 \rangle$; $C = \{\langle 024 \rangle, \langle 153 \rangle\}$; $D = \langle 01245 \rangle$; $E = \langle 0135 \rangle$; $F = \{\langle 03 \rangle, \langle 14 \rangle, \langle 25 \rangle\}$; $G = \langle 02514 \rangle$; $H = \{\langle 025 \rangle, \langle 014 \rangle\}$; $I = \langle 015 \rangle$; $J = \langle 15 \rangle$. The dashed lines are first-order boundaries.

We are particularly interested in the possible appearance of Υ points for finite D. An Υ point can occur when a first-order transition line separating, say, phases $\langle \alpha \rangle$ and $\langle \beta \rangle$ (that, for simplicity, we now assume to be nondegenerate) approaches a commensurate-incommensurate transition. An infinite number of phases spring out from the multicritical point at the end of the first-order line (as represented in Fig. 1). The phases appearing are made of sequences of $\langle \alpha \rangle$ and $\langle \beta \rangle$. As $\alpha \neq \beta$ the interfaces separating them, which we shall call $I_{\alpha\beta}$ and $I_{\beta\alpha}$ are also generally distinct. In the example of Fig. 1 the general form for a phase in the fan is $\langle \alpha^n I_{\alpha\beta} \beta^m I_{\beta\alpha} \rangle$, where the integers n, m increase approaching the $\langle \alpha \rangle$ and $\langle \beta \rangle$ boundaries, respectively.

The multiphase point **P** highlighted in Fig. 2 seems to be a good candidate for becoming an Υ point when D is relaxed from ∞. **P** lies at the end of a first-order transition line and it seems reasonable to consider the two multiphase lines J-G and G-F as special cases of accumulation lines. Therefore we might expect to observe a structure similar to Fig. 1 for small values of $1/D$.

III. $\langle \alpha \rangle$ BOUNDARY

Consider the J-G boundary (at a finite distance from the point **P**). When $D = \infty$ the phases $\langle \alpha \rangle \equiv \langle 51 \rangle$ (region J in Fig. 1) and $\langle 51402 \rangle$ (region G) coexist, and it is easy to check that along the boundary all phases built with α sequences separated by a $|402| \equiv I$ block (i.e., $\langle \alpha^n I \alpha^m ... \rangle$) are degenerate. We want to study how this degeneracy is lifted when D assumes finite values.

It is physically appealing to regard the I block of spins as an interface separating pure α sequences. Following Ref. 8 one can conveniently write the energy per spin of, say, phase $\langle \alpha^n I \rangle$ as

$$E = E_I^0 + [2n(E_\alpha^0 - E_I^0) + \sigma + V_\alpha(2n) + V_{\alpha\alpha}(2n, 2n) + \cdots]/(n_I + 2n), \tag{3.1}$$

where $n_I = 3$, E_I^0 (E_α^0) is the energy per spin of phase $\langle I \rangle$ ($\langle \alpha \rangle$), σ is the creation energy of I, $V_\alpha(2n)$ is the interaction energy of two interfaces I separated by a distance $2n$, $V_{\alpha\alpha}(2n, 2n)$ is the interaction energy of three interfaces, and so forth. In the $\langle \alpha \rangle$ region the interface tension σ is positive; as the phase boundary is approached σ decreases and eventually, when it balances the interface interactions, it will be favorable for the system to replace the pure α phase with a modulated one. The nature of the transition depends on the form of the interface interactions, which we now calculate to leading order using an expansion in inverse spin anisotropy.

In the large D limit $V_\alpha(2n)$ dominates the energy contribution from the interface interaction terms. It can be obtained using the reconnection formula[9]

$$V_\alpha(2n) = E_1 + E_2 - E_3 - E_4, \tag{3.2}$$

where E_i is the energy of configuration i as sketched in Fig. 3.

Equation (3.2) is exact, but is not convenient for our purposes, as we want only the leading term of $V_\alpha(2n)$. In fact, we can exploit the rapid decay of the V_α with n to substitute all infinite segments in Fig. 3 with finite (though sufficiently long) ones. Thus Eq. (3.2) can be approximated by

$$V_\alpha(2n) \approx E_A + E_B - E_C, \tag{3.3}$$

where A, B, and C, are the *periodic* configurations sketched in Fig. 4. $n_0 + 2n$ and $N - 2n - 2n_I - n_0$ are assumed to be both a large multiple of $2n$ and much greater than n_I.

We label the spins of configurations A, B, and C as $\{a_1, a_2, ..., a_{n_0} \equiv a_0\}$, $\{b_{n_0+1}, ..., b_N \equiv b_{n_0}\}$, and $\{c_1, c_2, ..., c_N \equiv c_0\}$, respectively. For D large the spins will deviate from their clock positions $\{a_i^0\}$, $\{b_i^0\}$, and $\{c_i^0\}$ by an angle analytic in D^{-1} and we write

$$a_i = a_i^0 + \tilde{a}_i, \qquad b_i = b_i^0 + \tilde{b}_i, \qquad c_i = c_i^0 + \tilde{c}_i. \tag{3.4}$$

We can choose to label the spins such that

$$a_i^0 = c_i^0, \qquad 1 \le i \le n_0, \quad b_i^0 = c_i^0, \qquad n_0 + 1 \le i \le N. \tag{3.5}$$

Then using a superscript tilde to indicate we are working only to second order in the spin deviations $\{\tilde{a}_i\}$, $\{\tilde{b}_i\}$, $\{\tilde{c}_i\}$ the two-interface interaction can be written

$$\begin{aligned}\tilde{V}_\alpha(2n) = {} & \tilde{\mathcal{H}}(\tilde{a}_{n_0}, \tilde{a}_1) + \sum_{i=2}^{n_0} \tilde{\mathcal{H}}(\tilde{a}_{i-1}, \tilde{a}_i) + \tilde{\mathcal{H}}(\tilde{b}_N, \tilde{b}_{n_0+1}) \\ & + \sum_{i=n_0+2}^{N} \tilde{\mathcal{H}}(\tilde{b}_{i-1}, \tilde{b}_i) \\ & - \tilde{\mathcal{H}}(\tilde{c}_N, \tilde{c}_1) + \sum_{i=2}^{N} \tilde{\mathcal{H}}(\tilde{c}_{i-1}, \tilde{c}_i),\end{aligned} \tag{3.6}$$

where

$$\begin{aligned}\tilde{\mathcal{H}}(\tilde{a}_{i-1}, \tilde{a}_i) = {} & J^a_{i-1,i}\{\tilde{a}_{i-1} - \tilde{a}_i + \Delta^a_{i-1,i}\}^2 \\ & + h^a_i(\tilde{a}_i + \epsilon^a_i)^2 + D\tilde{a}_i^2/2,\end{aligned} \tag{3.7}$$

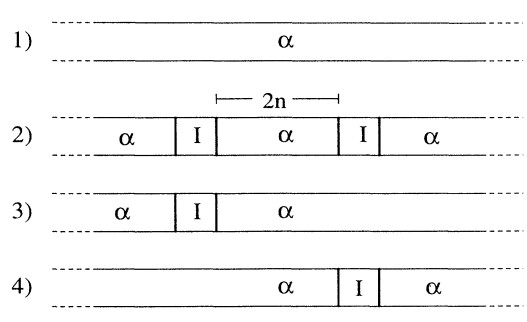

FIG. 3. Configurations needed to calculate the two-interface interaction; see Eq. (3.2).

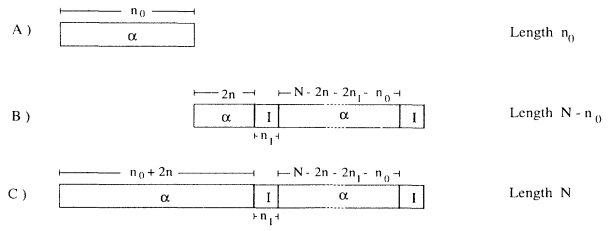

FIG. 4. Periodic configurations appearing in the approximate reconnection formula (3.3).

with

$$J^a_{i-1,i} = \cos(a^0_{i-1} - a^0_i + \pi\Delta/3)/2, \tag{3.8}$$

$$h^a_i = h\cos(a^0_i)/2, \tag{3.9}$$

$$\Delta^a_{i-1,i} = \tan(a^0_{i-1} - a^0_i + \pi\Delta/3), \tag{3.10}$$

$$\epsilon^a_i = \tan(a^0_i). \tag{3.11}$$

It follows from (3.5) that

$$\epsilon^a_i = \epsilon^b_i, \qquad h^a_i = h^b_i \tag{3.12}$$

for all i and that

$$J^a_{i-1,i} = J^c_{i-1,i}, \qquad \Delta^a_{i-1,i} = \Delta^c_{i-1,i}, \qquad 2 \le i \le n_0 \tag{3.13}$$

$$J^b_{i-1,i} = J^c_{i-1,i}, \qquad \Delta^b_{i-1,i} = \Delta^c_{i-1,i}, \qquad n_0 + 2 \le i \le N. \tag{3.14}$$

For the cases considered here it will be possible to label the phases so that (3.13) is also true for $i = 1$ and (3.14) for $i = n_0 + 1$. Under these circumstances we may drop the a, b, and c superscripts on the quantities defined in (3.8)–(3.11). It is then possible to use the recursion equations (2.2) to simplify (3.6). After some algebra one obtains

$$\begin{aligned}\tilde{V}_\alpha(2n) = {} & -J_{0,1}\{(\tilde{a}_{n_0} - \tilde{b}_N)(\tilde{c}_1 - \tilde{c}_{n_0+1}) \\ & -(\tilde{a}_1 - \tilde{b}_{n_0+1})(\tilde{c}_N - \tilde{c}_{n_0})\}.\end{aligned} \tag{3.15}$$

The quantities appearing in (3.15) can be obtained to leading order in $1/D$ using the recursion equation (2.2). An example of how to calculate $\tilde{V}_\alpha(2n)$ is given in the Appendix. The result for general n is

$$\tilde{V}_\alpha(2n) = C_2^n C_4^{n-1}\{S_4 - S_3\}^2/D^{2n} + \mathcal{O}(1/D^{(2n+1)}), \tag{3.16}$$

where

$$S_i \equiv \sin[\pi(\Delta - i)/3]\,, \tag{3.17}$$

$$C_i \equiv \cos[\pi(\Delta - i)/3]. \tag{3.18}$$

Terms of higher order than quadratic in the Hamiltonian (2.1) will not contribute to the leading term of the interface-interface interaction and hence to leading order $V_\alpha(2n)$ and $\tilde{V}_\alpha(2n)$ will be equal. Therefore we shall not distinguish between them below.

A knowledge of the leading term in the interface-interface interaction, Eq. (3.16), allows us to take the first

step in determining the ground-state configurations. Because we are considering only two-interface interactions the interfaces must be equispaced in the ground state. Inspection of Eq. (3.16) shows that $V_\alpha(2n)$ is always positive and convex near **P**. This is enough to conclude that, for D large, all transitions $\langle\alpha^n I\rangle \to \langle\alpha^{n+1} I\rangle$ occur as σ is lowered.[8]

To this order of approximation the $\langle\alpha^n I\rangle : \langle\alpha^{n+1} I\rangle$ phase boundaries remain degenerate and higher-order interface interactions can introduce qualitative changes in the phase diagram. This will be discussed further in Sec. V.

IV. $\langle\beta\rangle$ BOUNDARY

We now focus our attention on what happens along the $\langle\beta\rangle$ boundary in the two-interface interaction approximation. In the F region of the phase diagram (Fig. 2) three phases coexist when $D = \infty$, namely $\beta_1 = \langle 14\rangle$, $\beta_2 = \langle 25\rangle$, and $\beta_3 = \langle 03\rangle$. However, when D is relaxed, only phases β_1 and β_2 continue to stay degenerate, while phase β_3 has a higher energy.

Consider the boundary between one of the phases $\langle\alpha^n I\rangle$ and region F. Along this boundary, in the absence of interactions between the interfaces $I_1 \equiv (51)^n 4$, $I_2 \equiv 0$, and $I_3 \equiv 2$, all phases $\langle (51)^n 4(14)^{m_1} 0(30)^{l_1} 2(52)^{p_1} (51)^n 4(14)^{m_2} 0(30)^{l_2} 2(52)^{p_2} \ldots.\rangle$ are degenerate.

Now we turn on the two-interface interactions. In this approximation, the possible ground states are periodic and have the form $\langle (51)^n 4(14)^m 0(30)^l 2(52)^p\rangle$, where m, l, and p depend on σ. In the following analysis we shall hold n fixed and assume that σ can be varied to trace out the phase sequences.

The energy per spin can be written

$$E = \Big\{(1+2n)E_{I_1} + E_{\beta_1} 2m + E_{I_2} + E_{\beta_2} 2p + E_{I_3} + E_{\beta_3} 2l + \sigma + V_{\beta_1}(2m) + V_{\beta_3}(2l) + V_{\beta_2}(2p)\Big\}/L, \tag{4.1}$$

where $L = (2m+2p+2l+3+2n)$ and σ includes the energy tension of the three interfaces I_1, I_2, and I_3. Simple calculations show that

$$E_{\beta_1} = E_{\beta_2}, \quad E_{\beta_3} = E_{\beta_2} + 3h^2/(8D) + \mathcal{O}(1/D^2). \tag{4.2}$$

Proceeding as in Sec. III and the Appendix the two-wall interactions between interfaces bounding phases $\langle\beta_1\rangle$, $\langle\beta_2\rangle$, and $\langle\beta_3\rangle$ are to leading order

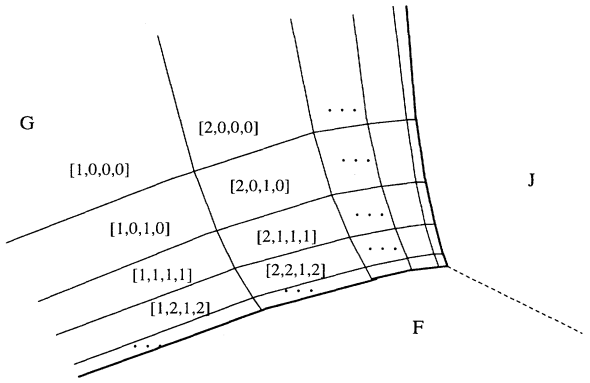

FIG. 5. Schematic phase diagram near the Υ point in the two-interface interaction approximation. The notation $[n,m,l,p]$ is used to indicate the phase $\langle (51)^n 4(14)^m 0(30)^l 2(52)^p\rangle$. The bold solid lines are accumulation lines. The dashed line is a first-order boundary.

$$V_{\beta_1}(2m) = V_{\beta_2}(2p) = D^{-(2m+2)}\{S_2 - S_3\}^2 C_3^{2m+1},$$
$$V_{\beta_3}(2l) = DV_{\beta_1}(2l)/C_3. \tag{4.3}$$

We now want to find the values $\bar{m}$, $\bar{p}$, and $\bar{l}$ which minimize (4.1) for a given n and σ. By symmetry arguments one has $\bar{m} = \bar{p}$. It follows from (4.2) that $\bar{l}$ must be bounded from above. Indeed an explicit calculation of the energy $\mathcal{O}(1/D)$ shows immediately that $\bar{l} = 0$ or 1 and that the sequence of phases as σ is lowered is, using the notation $[\bar{n},\bar{m},\bar{l},\bar{p}]$, $[\bar{n},0,0,0] \to [\bar{n},0,1,0] \to$ F.

The boundary between $[\bar{n},0,0,0]$ and $[\bar{n},0,1,0]$ is nondegenerate and cannot be split by terms of higher order in D^{-1}. The boundary between $[\bar{n},0,1,0]$ and F remains degenerate to all phases of the form $[\bar{n},m,1,m]$. The effect of higher-order terms can be deduced by noting that $V_{\beta_1}(2m)$ and $V_{\beta_2}(2p)$ are positive and convex. This implies that all the transitions $[\bar{n},m,1,m] \to [\bar{n},m+1,1,m+1]$ are stable.[8] Figure 5 summarizes the results of the two-interface interaction analysis.

V. HYPERFINE STRUCTURE

We now restrict our analysis to the richest region of the phase diagram, i.e., where $l = 1$. We already know that, in the two-interface approximation, the possible ground states can be written in the form $\langle\alpha^n I_1 \beta_1^m I_2 \beta_2^m I_3\rangle \equiv [n,m,m]$, where $I_1 \equiv 4$, $I_2 \equiv 030$, and $I_3 \equiv 2$. Bassler, Sasaki, and Griffiths[9] have shown that for exponentially decaying interactions such as is the case here the general form of the interaction energy of an arbitrary number of interfaces can be constructed as

$$V_{\alpha\beta_1\beta_2\ldots\beta_2}(2n,2m,2p,2q,\ldots,2s) = V_\alpha(2n) t_{\alpha\beta_1} V_{\beta_1}(2m) t_{\beta_1\beta_2} V_{\beta_2}(2p) t_{\beta_2\alpha} V_\alpha(2q) \ldots t_{\beta_1\beta_2} V_{\beta_2}(2s), \tag{5.1}$$

where the V's are defined in (3.16) and (4.3) and to leading order we find

$$t_{\beta_1\beta_2} = D^{-3}\{S_2 - S_3\}^{-2}C_2^2C_3^2,$$
$$t_{\alpha\beta_1} = D\{(S_3 - S_2)(S_4 - S_3)\}^{-1},$$
$$t_{\beta_2\alpha} = t_{\alpha\beta_1}. \tag{5.2}$$

The formulas (5.2) follow from calculations similar to that described in the Appendix. For example, taking the phases $A = [n, m, m]$, $B = [n, m+1, m+1]$, and $C = [n, m, m, n, m+1, m+1]$ the right-hand side of Eq. (3.15) is equal in leading order to $V_{\beta_1}(2m)t_{\beta_1\beta_2}V_{\beta_2}(2m+2)$. $t_{\beta_1\beta_2}$ can then immediately be extracted by using the expression (4.3) for V_{β_1} and V_{β_2}.

With the aid of (5.1) it is possible to examine the effects of three-interface interactions on the superdegenerate boundaries in Fig. 5. Consider the general case represented in Fig. 6(a). All four boundaries are multiphase lines where any sequence of the two neighboring phases are degenerate within the two-interface interaction approximation. For the $[n, m, m] : [n+1, m, m]$ and $[n, m+1, m+1] : [n+1, m+1, m+1]$ boundaries

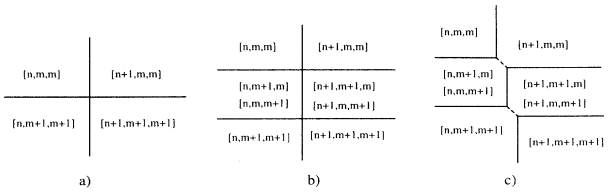

FIG. 6. Detail of the phase diagram in (a) the two-interface approximation; (b) the three-interface approximation; (c) the four-interface approximation. First-order lines are dashed.

this exhausts the possibilities and the three-interface interactions are not of sufficiently long range to split the degeneracy. For the $[n, m, m] : [n, m+1, m+1]$ ($[n+1, m, m] : [n+1, m+1, m+1]$) boundary, however, the phases $[n, m+1, m]$ and $[n, m, m+1]$ ($[n+1, m+1, m]$ and $[n+1, m, m+1]$) are also degenerate and there is the possibility that these may be stabilized with respect to $[n, m, m]$ and $[n, m+1, m+1]$ ($[n+1, m, m]$ and $[n+1, m+1, m+1]$) by the three-interface interaction.

To check this we need the energy differences[8,9]

$$\begin{aligned} 2E_{[n,m+1,m]} - E_{[n,m,m]} - E_{[n,m+1,m+1]} &= 2E_{[n,m,m+1]} - E_{[n,m,m]} - E_{[n,m+1,m+1]} \\ &\sim V_{\beta_1\beta_2}(m, m+1) + V_{\beta_1\beta_2}(m+1, m) - V_{\beta_1\beta_2}(m+1, m+1) - V_{\beta_1\beta_2}(m, m), \end{aligned} \tag{5.3}$$

which are dominated by $V_{\beta_1\beta_2}(m, m)$ and which are therefore negative. Similarly the $[n+1, m, m] : [n+1, m+1, m+1]$ boundary is unstable with respect to the formation of $\{[n+1, m+1, m], [n+1, m, m+1]\}$. The resulting modification to the phase diagram is sketched in Fig. 6(b).

The V_4 terms do not cause further splitting of the multidegenerate lines of Fig. 6(b) but they qualitatively change the phase diagram near the two points where four lines meet. In proximity of the upper one the structure of the phase diagram is determined by the signs of the energy differences[9]

$$\Delta V_1 = V_{\alpha\beta_1\beta_2}(n, m, m) + V_{\alpha\beta_1\beta_2}(n+1, m+1, m) - V_{\alpha\beta_1\beta_2}(n+1, m, m) - V_{\alpha\beta_1\beta_2}(n, m+1, m),$$
$$\Delta V_2 = V_{\beta_1\beta_2\alpha}(m, m, n) + V_{\beta_1\beta_2\alpha}(m+1, m, n+1) - V_{\beta_1\beta_2\alpha}(m+1, m, n) - V_{\beta_1\beta_2\alpha}(m, m, n+1). \tag{5.4}$$

With the aid of the factorization formulas (5.1) it is possible to check that the two energy differences (5.4) are positive. This means that phases $[n+1, m, m]$ and $\{[n, m, m+1], [n, m+1, m]\}$ are separated by a short first-order line; similarly one can show that $\{[n+1, m, m+1], [n+1, m+1, m]\}$ and $[n, m+1, m+1]$ also coexist at a first-order transition. In this approximation the structure of Fig. 6(b) must be modified as in Fig. 6(c).

The factorization formulas (5.1) allow us to go further and study the effect on the phase diagram of interface-interface interactions of all orders. Bassler, Sasaki, and Griffiths[9] showed that the form of the phase diagram depends upon the sign of the two-interface interactions (3.16) and (4.3) and the t's, Eq. (5.2). Here these are all positive corresponding to a case where the superdegenerate boundaries at the end of the first-order lines in Fig. 6(c) split under the effect of higher-order interface-interface interactions, giving rise to a structure analogous to that in Fig. 5 (but where the phases have longer periodicity). Furthermore one can carry the analysis further

by studying again the splitting near the points where four lines meet and so on, finding a structure similar to the one in Fig. 6(c). The analysis can then be repeated ad infinitum, showing that the Υ point has, indeed, a self-similar, fractal structure.

VI. DISCUSSION

The analysis presented above was based on retaining only the leading-order term in the interface-interface interaction. We cannot rule out the possibility that the neglected higher-order contributions could affect the phase diagram. In particular there will be correction terms $\mathcal{O}(l^2/D^2)$ where l is the period of a given phase which could introduce qualitative changes for l large and D not sufficiently small.

The results were checked numerically in two ways. First we used the Floria-Griffiths algorithm[10] on a grid of size 1200 to check which phases appeared. It was possible to resolve phases with l up to 13. Secondly we used a mean-field analysis, exact at zero temperature, to check the positions of the phase boundaries. In this way the formulas for the interface-interface interactions could be verified for short-period phases (typically l up to 9).

To summarize, we have presented analytic evidence for the existence of an Υ point in a spin model. The phase diagram has been constructed inductively by calculating the interface-interface interactions to leading order in $1/D$, the inverse spin anisotropy. Following arguments due to Bassler, Sasaki, and Griffiths[9] we have argued that the Υ point has a self-similar, fractal structure.

ACKNOWLEDGMENTS

J.M.Y. acknowledges the financial support of EPSRC and C.M. acknowledges the financial support of EPSRC and a grant from the Fondazione "A. della Riccia," Firenze. We thank Professor R.B. Griffiths for helpful discussions.

APPENDIX: CALCULATION OF THE TWO-INTERFACE INTERACTION

As an example of how to obtain the two-interface interaction we consider explicitly the calculation of $\tilde{V}_\alpha(6)$. Following Fig. 4 we need to consider the periodic phases listed below where $n_0 = 4$, $N = 24$, and $n = n_I = 3$. A choice of labeling that satisfies (3.13) for $1 \le i \le n_0$ and (3.14) for $n_0 + 1 \le i \le N$ is as shown:

$$
\begin{array}{lll}
 & & i = n_0;\ 1,\ 2,\ \ldots \\
 & & \quad\ \downarrow\ \downarrow \\
A: & 3a_i^0/\pi & \quad 5\ \ 1\ \ 5\ \ 1 \\
 & & i = \ldots\ N; n_0+1,\ \ \ldots \\
 & & \quad\ \downarrow\ \downarrow \\
B: & 3b_i^0/\pi & \quad 5\ \ 1\ \ 5\ 1\ 5\ \ 1\ 4\ 0\ 2\ 5\ 1\ 5\ 1\ 5\ 1\ 5\ 1\ 4\ 0\ 2 \\
 & & i = N;\ 1,\ \ \ldots\ \ \ n_0, n_0+1,\ \ldots \\
 & & \quad\ \downarrow\ \downarrow\ \ \ \ \ \ \downarrow\ \downarrow \\
C: & 3c_i^0/\pi & \quad 5\ \ 1\ \ 5\ 1\ 5\ \ 1\ 5\ 1\ 5\ \ 1\ 4\ 0\ 2\ 5\ 1\ 5\ 1\ 5\ 1\ 5\ 1\ 4\ 0\ 2\,. \qquad \text{(A1)}
\end{array}
$$

We can now use (3.15) to calculate $\tilde{V}_\alpha(6)$ to leading order. The quantities $(\tilde{a}_{n_0} - \tilde{b}_N)$, $(\tilde{a}_1 - \tilde{b}_{n_0+1})$, $(\tilde{c}_1 - \tilde{c}_{n_0+1})$, and $(\tilde{c}_N - \tilde{c}_{n_0})$ can be obtained correct to leading order from the linear approximation to the recursion equation (2.2),

$$
\tilde{\theta}_i = \Big\{ -2h_i^\theta(\epsilon_i^\theta + \tilde{\theta}_i) + 2J_{i-1,i}^\theta(\tilde{\theta}_{i-1} - \tilde{\theta}_i + \Delta_{i-1,i}^\theta) - 2J_{i,i+1}^\theta(\tilde{\theta}_i - \tilde{\theta}_{i+1} + \Delta_{i,i+1}^\theta) \Big\}/D, \qquad \text{(A2)}
$$

where we have used the definitions (3.8)–(3.11).

Let

$$
\tilde{\theta}_i = \frac{\theta_i^1}{D} + \frac{\theta_i^2}{D^2} + \cdots . \qquad \text{(A3)}
$$

Substituting into (A2) and equating like powers of D^{-1} gives

$$
\theta_i^1 = 2J_{i-1,i}^\theta \Delta_{i-1,i}^\theta - 2J_{i,i+1}^\theta \Delta_{i,i+1}^\theta - 2h_i^\theta \epsilon_i^\theta, \qquad \text{(A4)}
$$

$$
\theta_i^n = -2h_i^\theta \theta_i^{n-1} - 2J_{i-1,i}^\theta(\theta_{i-1}^{n-1} - \theta_i^{n-1}) - 2J_{i,i+1}^\theta(\theta_i^{n-1} - \theta_{i+1}^{n-1}), \qquad n > 1. \qquad \text{(A5)}
$$

To calculate $(\tilde{a}_1 - \tilde{b}_{n_0+1})$ it is helpful to display explicitly a_i^0 and $b_{n_0+i}^0$ as a function of i:

$$
\begin{array}{lcccccccccccccc}
i & \ldots & -3 & -2 & -1 & 0 & & 1 & 2 & 3 & 4 & \ldots \\
 & & * & & & & & & & & * & \\
3a_i^0/\pi & \ldots & 5 & 1 & 5 & 1 & 5 & : & 1 & 5 & 1 & 5 & 1 \ldots \\
3b_{n_0+i}^0/\pi & \ldots & 0 & 2 & 5 & 1 & 5 & : & 1 & 5 & 1 & 4 & 0 \ldots \\
 & & & * & & & & & & & & * &
\end{array}
\tag{A6}
$$

The $*$'s mark where a_i^0 first differs from $b_{i+n_0}^0$ when moving away from the dotted interface in either direction.

It follows immediately from (A4) that

$$
(\tilde{a}_3 - \tilde{b}_{n_0+3}) = \frac{1}{D}\left\{\sin\left[\frac{\pi}{3}\Delta - 3\right] - \sin\left[\frac{\pi}{3}\Delta - 4\right]\right\}. \tag{A7}
$$

Two further iterations of (A5) give

$$
\begin{aligned}
(\tilde{a}_1 - \tilde{b}_{n_0+1}) &= \frac{1}{D^2}\cos\left[\frac{\pi}{3}\Delta + a_1^0 - a_2^0\right]\cos\left[\frac{\pi}{3}\Delta + a_2^0 - a_3^0\right](\tilde{a}_3 - \tilde{b}_{n_0+3}) \\
&= \frac{1}{D^3}\cos\left[\frac{\pi}{3}(\Delta - 4)\right]\cos\left[\frac{\pi}{3}(\Delta - 2)\right]\left\{\sin\left[\frac{\pi}{3}\Delta - 3\right] - \sin\left[\frac{\pi}{3}\Delta - 4\right]\right\}.
\end{aligned} \tag{A8}
$$

$(\tilde{a}_{n_0} - \tilde{b}_N)$ may be calculated in an analogous way

$$
(\tilde{a}_{n_0} - \tilde{b}_N) = -(\tilde{a}_1 - \tilde{b}_{n_0+1}). \tag{A9}
$$

Similarly

$$
(\tilde{c}_1 - \tilde{c}_{n_0+1}) = (\tilde{c}_N - \tilde{c}_{n_0}) = (\tilde{a}_1 - \tilde{b}_{n_0+1}). \tag{A10}
$$

Using $J_{0,1} = \cos[\frac{\pi}{3}(\Delta - 2)]/2$, from the definition (3.8) and substituting (A8)–(A10) into (3.15) gives

$$
\tilde{V}_\alpha(6) = -\frac{1}{D^6}\left\{\sin\left[\frac{\pi}{3}\Delta - 4\right] - \sin\left[\frac{\pi}{3}\Delta - 3\right]\right\}^2 \cos\left[\frac{\pi}{3}(\Delta - 4)\right]^2 \cos\left[\frac{\pi}{3}(\Delta - 2)\right]^3. \tag{A11}
$$

It is important to point out that the labeling used in Eq. (A1) is not unique. Any labeling which satisfies (3.13) for $1 \le i \le n_0$ and (3.14) for $1 \le n_0+1 \le N$ will give the correct results for $\tilde{V}_\alpha(6)$. However, in general $(\tilde{a}_1 - \tilde{a}_{n_0+1})$, etc. will contain lower powers of $1/D$ which cancel when the difference in (3.15) is taken. The choice given above, which maximizes the distance of the position $(*)$ where a_i^0 first differs from $b_{n_0+1}^0$ avoids such cancellation and leads to the easiest calculation.

It is important to mention that because the interface-interface interactions decay very rapidly (exponentially) with increasing interface-interface distance the values of $n_0 + 2n$ and $N - 2n - 2n_I - n_0$ need not in fact be much larger that $2n$ and n_I. That sufficiently large values have been chosen can be checked *a posteriori* by verifying that increasing the values of n_0 and N does not change the result (A11).

Finally we give an explicit expression for the interface energy σ defined in (3.1). A leading-order calculation gives

$$
\begin{aligned}
\sigma = C_2 + C_4 - 2C_3 + \frac{1}{D}\{&S_2^2 - 2S_3^2 - 2S_2S_4 + 4S_3S_4 - S_4^2 \\
&+ h\sqrt{3}(S_2 - 2S_3 + S_4)\} + \mathcal{O}(D^{-2}) .
\end{aligned} \tag{A12}
$$

[1] M. E. Fisher and W. Selke, Phys. Rev. Lett. **44**, 1502 (1980).
[2] A. B. Harris, C. Micheletti, and J. M. Yeomans, Phys. Rev. Lett. **74**, 3045 (1995).
[3] F. Seno and J. M. Yeomans, Phys. Rev. B **50**, 10 385 (1994) and (unpublished).
[4] W. Chou and R. B. Griffiths, Phys. Rev. B **34**, 6219 (1986).
[5] K. Sasaki and L. M. Floria, J. Phys. Condens. Matter **1**, 2179 (1989).
[6] K. Sasaki, J. Stat. Phys. **68**, 1013 (1992).
[7] C. S. O. Yokoi, L. H. Tang, and W. R. Chou, Phys. Rev. B **37**, 2173 (1988).
[8] M. E. Fisher and A. M. Szpilka, Phys. Rev. B **36**, 644 (1987).
[9] K. E. Bassler, K. Sasaki, and R. B. Griffiths, J. Stat. Phys. **62**, 45 (1991).
[10] L. M. Floria and R. B. Griffiths, Numer. Math. **55**, 565 (1989).